Published in final edited form as:
Biochemistry. 2013 September 17; 52(37): . doi:10.1021/bi400682n.

Interaction of profilin with the barbed end of actin filaments

Naomi Courtemanche[1] and **Thomas D. Pollard**[1,2,3,*]

[1]Department of Molecular Cellular and Developmental Biology, Yale University, PO Box 208103, New Haven, CT 06520-8103 USA

[2]Department of Molecular Biophysics and Biochemistry, Yale University, PO Box 208103, New Haven, CT 06520-8103 USA

[3]Department of Cell Biology, Yale University, PO Box 208103, New Haven, CT 06520-8103 USA

Abstract

Profilin binds not only to actin monomers but also to the barbed end of the actin filament, where it inhibits association of subunits. To address open questions about the interactions of profilin with barbed ends, we measured the effects of a wide range of concentrations of *Homo sapiens* profilin 1 on the rate of elongation of individual skeletal muscle actin filaments by total internal reflection fluorescence microscopy. Much higher concentrations of profilin were required to stop elongation by AMP-PNP-actin monomers than ADP-actin monomers. High concentrations of profilin depolymerized barbed ends much faster than the spontaneous dissociation rates of Mg-ATP-, Mg-AMP-PNP-, Mg-ADP-P_i- or Mg-ADP-actin subunits. Fitting a thermodynamic model to these data allowed us to determine the affinities of profilin and profilin-actin for barbed ends and the influence of the nucleotide bound to actin on these interactions. Profilin has a much higher affinity for ADP-actin filament barbed ends (K_d = 1 μM) than AMP-PNP-actin filament barbed ends (K_d = 226 μM). ADP-actin monomers associated with profilin bind to ADP-actin filament barbed ends 10% as fast as free ADP-actin monomers, but bound profilin does not affect the rate of association of AMP-PNP-actin monomers with barbed ends. The differences in the affinities of AMP-PNP- and ADP-bound barbed ends for profilin and profilin-actin suggest that conformations of barbed end subunits differ from those of monomers and change upon nucleotide hydrolysis and phosphate release. A structural model revealed minor steric clashes between profilin and actin subunits at the barbed end that explain the biochemical results.

The small protein profilin performs many roles in cytoskeletal dynamics through interactions with actin monomers, poly-L-proline ligands including formins, and the barbed ends of actin filaments (1). Understanding the mechanism of action of profilin has proven to be remarkably challenging for such a small protein (125–137 amino acids). Profilin binds actin monomers and inhibits spontaneous assembly of actin polymers (2–5), so the initial hypothesis was that profilin sequesters actin monomers, so they cannot polymerize. Low concentrations of profilin strongly inhibit actin filament nucleation (2–4) and elongation of actin filament pointed ends (6). Both effects are due to profilin binding to the barbed end of the actin monomer with micromolar affinity and physically blocking association of the complex with pointed ends during nucleation and elongation (7, 8).

[*]Correspondence: thomas.pollard@yale.edu, (203) 432-3565.

Supporting Information Available

Supplemental Table S1 lists reaction rates and affinities for ATP-actin and profilin. Supplemental Figure S1 shows the dependence of R^2-values of fits obtained from our data analysis on the absolute value of K_{d4} for AMP-PNP-actin and ADP-P_i-actin. Supplemental Figure S2 shows the depolymerization of representative ATP-actin filament barbed ends in the presence of profilin. This material is available free of charge via the Internet at http://pubs.acs.org.

On the other hand, events at the barbed end of actin filaments are less clear (9). Saturating ATP-actin monomers with profilin has little effect on the elongation of actin filament barbed ends, but since high concentrations of profilin slow elongation (6, 10), profilin was proposed to bind weakly to barbed ends, thereby blocking association of subunits on the barbed end. If this filament capping mechanism is correct, theory predicts that high concentrations of profilin will stop and reverse barbed end elongation (11). Although this was not achieved with the highest profilin concentrations used in initial studies done in the presence of actin monomers (6) (12–18), high concentrations of profilin depolymerized aged filaments assembled from ATP-actin and observed with DNase-I bound to actin monomers in solution (15) or diluted to lower the concentration of monomers (19). These filaments were assumed to be composed of ADP-actin subunits. Recent elegant experiments confirmed that profilin depolymerizes individual aged actin filaments in a concentration-dependent manner (20). However, these experiments did not include actin monomers, so the rates of profilin binding and dissociation at barbed ends, the rate of dissociation of profilin-actin from barbed ends and the overall thermodynamics of the system remained to be determined (9).

Here we used fluorescence microscopy to test the effects of a wide range of concentrations of human profilin 1 on the elongation of skeletal muscle actin filaments by Mg-ATP-, Mg-AMP-PNP-, Mg-ADP-P_i- or Mg-ADP-actin subunits. Low concentrations of profilin inhibited elongation of actin filament barbed ends and high concentrations of profilin caused barbed ends to depolymerize at rates much faster than spontaneous dissociation rates. A thermodynamic analysis of the dependence of elongation rates on profilin concentration yielded the affinities of profilin for barbed ends and the influence of the nucleotide bound to actin on its interactions with profilin. Profilin has a relatively high affinity (K_d = 1 μM) for ADP-actin filament barbed ends and a low affinity (K_d = 226 μM) for AMP-PNP-actin filament barbed ends, opposite to the relative affinities of profilin for actin monomers with these bound nucleotides. Association of profilin with actin monomers slows the association of ADP-actin monomers with barbed ends but has no effect on the rate of association of AMP-PNP-actin monomers with barbed ends. Profilin bound to a barbed end increases the dissociation rate of the terminal subunit.

Materials and Methods

Actin purification and labeling—Muscle actin was purified from an acetone powder of frozen chicken skeletal muscle (Trader Joe's) using one cycle of polymerization and depolymerization followed by gel filtration on Sephacryl S-300 and storage in Ca-Buffer-G (2 mM Tris-HCl, pH 8.0, 2 mM ATP, 0.1 mM $CaCl_2$, 1 mM NaN_3, 0.5 mM DTT) (21). The concentration of actin was measured by absorbance at 290 nm with an extinction coefficient of 26,600 $M^{-1}cm^{-1}$ (22). Muscle actin filaments in 50 mM PIPES, pH 6.8, 50 mM KCl, 0.2 mM $CaCl_2$, 0.2 mM ATP were labeled on lysines by incubating overnight at 4°C with a 1:13 molar ratio of actin to Alexa Fluor 488 carboxylic acid succinimidyl ester (A-20000, Invitrogen, Carlsbad, CA) (23). After depolymerization, clarification and gel-filtration on Sephacryl S-300, purified actin monomers were typically ~30–50% labeled. Ca-ATP-actin was converted to Mg-ATP-actin by adding 0.1 volumes of 2 mM EGTA and 500 μM $MgCl_2$ and incubating for 5 min at room temperature. Ca-ATP-actin monomers in Ca-Buffer-G were converted to Mg-ADP-actin monomers by incubating with 50 μM $MgCl_2$, 250 μM EGTA, 1 mM glucose and 0.25 units/mL of hexokinase (Sigma, St. Louis, MO, H-2005) for 3 h on ice followed by clarification for 1 h at 125,000 × G (24). Mg-ADP-P_i-actin solutions were generated during total internal reflection microscopy experiments by mixing Mg-ADP-actin monomers with ADP-P_i-TIRF buffer containing 12.5 mM potassium phosphate. Mg-AMPPNP-actin monomers were generated by two rounds nucleotide exchange with AG 1-

X4 resin (Bio-Rad, Hercules, CA) followed by incubation with 1 mM AMPPNP (A-2647, Sigma, St. Louis, MO) for 30 min at room temperature.

Profilin purification—*H. sapiens* profilin 1 was expressed in *E. coli* BL21 (pLysS) using a pMW172 plasmid (25) and purified by affinity chromatography on poly-L-proline coupled to Sepharose 4 Fast Flow (17-0981-01, Amersham Pharmacia, Piscataway, NJ) (26, 27). We used an extinction coefficient of 15,000 $M^{-1}cm^{-1}$ at λ = 280 nm to measure the concentration of profilin.

Microscopy and data analysis—Open-ended glass flow chambers were prepared as described (28). Before introduction of actin, each chamber was incubated for 1 min with two washes of 8 μL of 0.5% Tween-80 in high-salt TBS (HS-TBS) (50 mM Tris-HCl, pH 7.5, 600 mM KCl), followed by two washes with 10 μL of HS-TBS, two 30 s incubations with 8 μL of 250 nM NEM-inactivated skeletal muscle myosin, two washes with 10 μL of HS-TBS and two 30 s incubations with 8 μL of 10% BSA (w/v) in HS-TBS.

The standard microscopy buffer consisted of 10 mM imidazole, pH 7.0, 50 mM KCl, 1.0 mM EGTA, 1 mM $MgCl_2$, 1 mM EGTA, 15 mM glucose, 50 mM DTT, 0.02 μM $CaCl_2$, 20 μg/mL catalase, 100 μg/mL glucose oxidase, 0.5% methylcellulose (4,000 cP at 2% (w/v)) and an appropriate nucleotide: 0.3 mM ATP for ATP-actin; 0.37 mM AMPPNP for AMPPNP-actin; 0.3 mM ADP and 10 units/mL of hexokinase for ADP-actin; or 0.4 mM ADP, 12.5 mM potassium phosphate and 20 units/mL of hexokinase for ADP-P_i-actin.

Polymerization was initiated by introducing actin in microscopy buffer into the chamber. Upon appearance of short filaments, the solution in the chamber was replaced with a fresh sample of proteins (actin, actin plus profilin, or profilin alone) in microscopy buffer and imaging was continued.

We generated time-lapse movies of growing or shortening actin filaments using prism-style total internal reflection fluorescence microscopy on an Olympus IX70 inverted microscope and a Hamamatsu C4742-95 CCD camera controlled by MetaMorph software (Molecular Devices, Downingtown, PA) (29). Specimens were illuminated for 0.5–1 s at intervals of 5, 10 or 20 s depending on the rates of growth or shortening. Images were processed with ImageJ software (http://rsbweb.nih.gov/ij/). For each sample, we measured the rates of barbed end elongation of 10–15 filaments, typically over a span of at least 300 s.

Molecular models of profilin binding to actin filament barbed ends—The structure of human profilin 1 (pdb: 1FIK) was superimposed and compared to that of bovine profilin bound to bovine β-actin (pdb: 1HLU). The secondary structures were then used to superimpose the actin in this model onto the two terminal subunits of an actin filament (30) to look for steric clashes between profilin and subunits within the filament. Molecular models were constructed using the program superpose (31) and other tools from the CCP4 software suite (32). Solvent excluded surfaces were constructed using the program MSMS with a probe radius of 1.4 angstroms (33). Figures were made using Molscript (34) and Raster3D (35).

Theory

In a system with actin monomers, profilin and actin filaments, one must consider 4 reactions (Figure 1), identical to those used by Kinosian et al. in their analysis (15).

Reaction of profilin with actin monomers—The interaction of profilin (P) with an actin monomer (A) is a simple bimolecular reaction of profilin with the barbed end of an actin monomer, creating a 1:1 profilin-actin (PA) complex.

$$A+P \leftrightarrows PA \quad \text{Reaction 1}$$

The rate and equilibrium constants (K_{d1}) are known for each actin-nucleotide species (Table 2). The affinity of profilin for ATP-actin in polymerization buffer is reasonably high (K_d = 0.1 μM) and the exchange rate is fast (1.3 s^{-1}; (36)). The affinity of profilin for ADP-actin is about 6-fold lower.

Reaction of actin monomers with the barbed ends of actin filaments—Free actin monomers can bind and dissociate at both the barbed end (BE) and pointed end (PE), although the rates of the reactions differ. The association reaction converts an actin monomer (A) into a filamentous actin subunit (F) and the dissociation reaction converts a filamentous subunit (F) into a monomer (A). These reactions only occur at the ends of filaments, which act as catalysts and are not consumed. For the purposes of this study, we only consider subunit addition at the barbed end.

$$A+BE \leftrightarrows F+BE \quad \text{Reaction 2}$$

The rate and equilibrium constants (K_{d2} = critical concentration) are known for ATP-, ADP-P_i- and ADP-actin (Table 2). We measured these constants for AMP-PNP-actin in this study.

Reaction of profilin with actin filaments—Profilin does not bind along the length of actin filaments in pelleting (12) or fluorescence anisotropy assays (37), but polymerization experiments (6, 10, 15, 18) suggested that profilin binds to the barbed ends but not the pointed ends of actin filaments. These results, combined with our structural analysis (see below, Figure 5), indicate that each filament has a single profilin binding site, located at the barbed end of the terminal subunit.

$$P+BE \leftrightarrows BE-P \quad \text{Reaction 3}$$

Neither the rate nor equilibrium constants (K_{d3}) are known for any actin-nucleotide species. Note that our structural analysis shows that a barbed end associated with profilin (BE-P) is capped, so it cannot bind an actin monomer or profilin-actin complex. Profilin can dissociate from the barbed end alone (reaction 3) or in association with an actin subunit (reaction 4).

Reaction of the profilin-actin complex with the barbed ends of filaments—Profilin-actin (PA) cannot bind to the pointed end, but associates with barbed ends.

$$PA+BE \leftrightarrows BE-PA \leftrightarrows F+BE-P \quad \text{Reaction 4}$$

This association reaction consumes a barbed end and adds a subunit (F) to the filament. Note that profilin can also dissociate on its own from BE-P yielding P and BE (reaction 3). We measured the rate constants for the dissociation of profilin-actin (PA) from barbed ends for four actin-nucleotide species (Table 1), but none of the association rate constants or equilibrium constants (K_{d4}) were known.

We used the dependence of the filament elongation rates on profilin concentration to estimate the missing equilibrium constants for the affinities of profilin (K_{d3}) and profilin-

actin (K_{d4}) for the barbed ends of filaments composed of subunits with different bound nucleotides. Equations 1–3 describe the evolution of the concentrations of filamentous actin (F), filament barbed ends (BE) and profilin (P) over time. These equations are based on reactions 1–4 and use the association and dissociation rate constants (k_n^+ and k_n^-) for reaction n:

$$\frac{dF}{dt}=k_2^+[BE][A]+k_4^+[BE][PA]-k_2^-[BE]-k_4^-[BE\bullet P] \quad \text{(Eq. 1)}$$

$$\frac{dBE}{dt}=k_3^-[BE\bullet P]+k_4^-[BE\bullet P]-k_3^+[BE][P]-k_4^+[BE][PA] \quad \text{(Eq. 2)}$$

$$\frac{dP}{dt}=k_1^-[PA]+k_3^-[BE\bullet P]-k_1^+[A][P]-k_3^+[BE][P] \quad \text{(Eq. 3)}$$

Our experimental conditions allowed us to use four simplifying assumptions. (i) The change in the concentration of polymerized actin over time is much smaller than the initial concentration of actin monomers, so the concentrations of actin (A), profilin (P) and profilin-actin (PA) were constant. (ii) The total concentration of profilin does not change over time, so the initial concentration of profilin, P_0, is equal to the sum of the concentrations of free, actin-bound and barbed end-bound profilin, P + PA + BE-P, at any given time. (iii) The number of barbed ends does not change over time, so the initial concentration of barbed ends, BE_0, is equal to the sum of the concentrations of free and profilin-bound barbed ends, BE + BE-P, at any time. This assumption is reasonable given that our measurements were made on individual filament barbed ends. (iv) The initial concentration of actin, A_0, is equal at any time to the sum of the concentrations of free actin (A), profilin-bound actin (PA) and actin that becomes filamentous (F) since the start of the experiment (not including pre-formed filaments).

Using equations 1–3 and our simplifying assumptions, we modified equation 1 to describe the filament elongation rate in terms of the initial concentrations of actin, profilin and barbed ends, dissociation equilibrium constants for reactions 2–4 (K_{dn}, defined as k_n^-/k_n^+ for reaction n) and the association rate constant for reaction 2 (k_2^+):

$$\frac{dF}{dt}=k_2^+BE_0\frac{A_0(K_{d3}+K_{d4})+P_0(K_{d2}-K_{d4})}{P_0+(K_{d3}+K_{d4})} \quad \text{(Eq. 4)}$$

The only unknowns are K_{d3} and K_{d4}.

Results

We used total internal reflection fluorescence microscopy (29, 38, 39) to investigate the effects of a wide range of concentrations of human profilin 1 on actin monomer association and dissociation rates at barbed ends of actin filaments with ATP, AMP-PNP-, ADP-P_i or ADP bound to the actin monomers (Figure 2). Analysis of these polymerization data and structural models showed that profilin inhibits elongation of barbed ends by binding the terminal subunit of the filament and blocking subunit addition.

Effect of the bound nucleotide on barbed end elongation and shortening rates in the absence of profilin

To analyze our experiments with profilin, we used published barbed end association and dissociation rate constants for ATP, ADP-P_i and ADP-actin monomers (39, 40). To determine association and dissociation rates for AMP-PNP-actin monomers, we visualized barbed end elongation rates over a range of monomer concentrations by total internal reflection fluorescence microscopy (Figure 3). Elongation rates were linearly proportional to the concentration of actin monomers up to 1.75 μM actin. The slope and intercept gave association and dissociation rate constants of 12.6 $\mu M^{-1}s^{-1}$ and 0.09 s^{-1}, and a K_d of 0.01 μM^{-1}. The elongation rate was higher than expected at 2.5 μM actin. However, in addition to elongating existing filaments, AMP-PNP-actin monomers spontaneously formed many more short filaments than ATP-actin monomers (not shown), indicating that nucleation is much more favorable with AMP-PNP-actin than ATP-actin. Annealing of the high concentration of short filaments with barbed ends may have contributed to the high elongation rate with 2.5 μM AMP-PNP-actin.

The rates of actin subunit dissociation from filament ends in the absence of profilin were known for filaments polymerized from ATP-, ADP-P_i- and ADP-actin monomers (39, 40). We determined the dissociation rate for AMP-PNP-actin by measuring the shortening of AMP-PNP-actin filaments after washing out the actin monomers with polymerization buffer alone (Table 1).

Effect of profilin on actin filament depolymerization in the absence of monomeric actin

To obtain the rates of profilin-actin dissociation from filament ends uncomplicated by association of profilin-actin with the ends, we measured shortening of filaments polymerized from ATP-, AMP-PNP-, ADP-P_i- or ADP-actin monomers after washing out the actin monomers with polymerization buffer containing 750 μM human profilin but without free actin monomers (Table 1). Under these conditions profilin should saturate the barbed ends, making profilin-actin the major species dissociating from the ends. As reported previously for ADP-actin (15), saturating profilin increased the rates that barbed ends shortened with the most dramatic effect on Mg-AMP-PNP-actin filaments and the smallest effect on Mg-ADP-actin filaments (Table 1). Although the depolymerization rate we measured in saturating profilin for Mg-ADP-P_i-actin filaments (−8.6 subunits/s) was similar to that reported by Jegou and coworkers (−4.7 subunits/s) (20), the rate we observed using Mg-ADP-actin filaments (−12.2 subunits/s) was only 30% that observed by Jegou and coworkers (−41 subunits/s). However, as discussed below, this range of depolymerization rates for Mg-ADP-actin does not affect our main conclusions.

Effect of profilin on elongation and shortening of actin filament barbed ends

To characterize interactions of profilin with the barbed ends of filaments, we observed actin filament elongation or shortening in profilin concentrations ranging from 10 to 150 μM for 1.5 μM Mg-ATP-actin, from 5 to 225 μM for 1.5 μM AMP-PNP-actin, from 2.5 to 300 μM for 4 μM ADP-P_i-actin and from 0.5 to 25 μM for 5 μM Mg-ADP-actin (Figure 4). Most filaments grew at steady rates throughout the observation times, interrupted in some cases by short, obvious pauses.

Profilin inhibited elongation of actin filament barbed ends in a concentration-dependent fashion. Stoichiometric concentrations of profilin stopped barbed end elongation with 5 μM ADP-actin (Figure 4D), whereas ~60 μM profilin was required to stop elongation in the presence of 1.5 μM ATP-actin (Figure 4A). Profilin concentrations higher than those required to stop elongation caused barbed ends to shorten, and short filaments eventually depolymerized and disappeared. A few barbed ends did not shorten immediately or paused

for 45–60 s as they depolymerized. Encounters of depolymerizing barbed ends with myosin attachment points may have contributed to these pauses, because barbed ends fluctuated laterally much less during pauses than before and after these delays. Alternatively, laser-induced subunit cross-linking may also have contributed to some pauses (41). Elongation rates fell on smooth curves at low and high profilin concentrations but not at intermediate profilin concentrations, (40–60 μM profilin for ATP-actin, 75–125 μM profilin for AMP-PNP-actin and 50–75 μM profilin for ADP-P_i-actin) where elongation rates were near zero (Figure 4A, B, C open circles). Long timescales were required to visualize these low rates of polymerization and depolymerization, so photocrosslinking events may have compromised the measurements. For this reason, we did not include these intermediate data points in our analysis (see below).

Effect of profilin on elongation of actin filament barbed ends by AMP-PNP-actin

Barbed end elongation rates with 1.5 μM Mg-AMP-PNP-actin monomers were close to zero with ~100 μM profilin (Figure 4B), 20-fold higher than the concentration required to stop elongation of barbed ends by Mg-ADP-monomers (Figure 4D). Profilin concentrations greater than 125 μM caused barbed ends to shorten. Given the low concentration of total AMP-PNP-actin monomers (1.5 μM) and their high affinity for profilin (K_{d1} = 0.1 μM), most AMP-PNP-actin monomers were bound to profilin at all profilin concentrations (5–225 μM) tested, so the main species that varied with total profilin concentration was the free profilin concentration. The experimental data in Figure 4B revealed that this free profilin was titrating a species with a very low affinity for barbed ends.

We fit our polymerization data using Equation 4 and extracted the affinities of profilin and profilin-AMP-PNP-actin for AMP-PNP-actin filament barbed ends using the association and dissociation rates summarized in Table 2. The results of our fitting indicate that the affinity of AMP-PNP-actin filament barbed ends for the profilin-AMP-PNP-actin complex (K_d = 4.6 μM) is 49-fold higher than for free profilin (K_d = 226 μM). The data strongly constrain the ratio of these two equilibrium constants, as demonstrated by a plot of the R^2-value of fits performed by fixing K_{d3} at 226 μM and varying the value of K_{d4} (Supplemental Figure S1A). Although a range of values of K_{d3} and K_{d4} fit the data reasonably well so long as their ratio remains the same, the particular combination of 226 and 4.6 μM provides the best fit to our data (not shown). Thus, association of the profilin-AMP-PNP-actin complex is the main pathway capping barbed ends and inhibiting elongation. Secondly, since profilin-AMP-PNP-actin and monomeric AMP-PNP-actin bind to barbed ends at similar rates, the large difference in their affinities arises from much faster dissociation of profilin-AMP-PNP-actin from barbed ends (which we measured directly). Free energy calculations for each of the binding reactions reveal that the thermodynamic parameters produced by our fitting are balanced (within 0.9 kcal/mol; Figure 1), and therefore these four reactions are sufficient to describe the polymerization of AMP-PNP-actin in the presence of profilin.

Effect of profilin on elongation of actin filament barbed ends by ADP-P_i-actin

Barbed end elongation rates with 4 μM Mg-ADP-P_i-actin monomers were zero with ~40 μM profilin (Figure 4C), ~2.5-fold lower than the profilin concentration required to stop elongation of barbed ends by Mg-AMP-PNP-monomers. Profilin concentrations ranging from 40 to 200 μM appeared to stall polymerization, perhaps owing to photocrosslinking events that accumulate during the long times required to visualize and measure small depolymerization rates. However, profilin concentrations >225 μM caused barbed ends to shorten. Given the high affinity of ADP-P_i-actin for profilin (K_{d1} = 0.1 μM), most of the ADP-P_i-actin monomers were bound to profilin at all profilin concentrations (2.5–300 μM) tested, so the main species that varied with total profilin concentration was the free profilin concentration.

Using Equation 4 to fit the ADP-P_i-actin polymerization data, we determined that the affinity of ADP-P_i-actin filament barbed ends is 5-fold higher for the profilin-ADP-P_i-actin complex than free profilin. As with our AMP-PNP-actin data, the ADP-P_i-actin polymerization data strongly constrain the ratio of these two equilibrium constants, as demonstrated by a plot of the R^2-value of fits performed by fixing K_{d3} at 10.2 μM and varying the value of K_{d4} (Supplemental Figure S1B). Although a range of values of K_{d3} and K_{d4} fit the data reasonably well so long as their ratio remains the same, the particular combination of 10.2 μM and 2.1 μM provides the best fit to our data (not shown). Thus both direct binding of profilin and association of profilin-ADP-P_i-actin contribute to capping barbed ends. Secondly, as we observed for AMP-PNP-actin, the association rate constants for monomeric ADP-P_i-actin and profilin-bound ADP-P_i-actin to barbed ends are similar, so the dissociation rate constants determine the affinities. Free energy calculations show that our thermodynamic parameters are balanced (within 0.6 kcal/mol) for the reactions involving ADP-P_i-actin (Figure 1).

Effect of profilin on elongation of actin filament barbed ends by ADP-actin

Low micromolar profilin concentrations inhibited elongation of barbed ends by 5 μM Mg-ADP-actin monomers, whereas profilin concentrations exceeding 5 μM depolymerized barbed ends (Figure 4C). Unconstrained fits to our elongation data produced negative dissociation equilibrium constants for reaction 3 (K_{d3}). To correct this problem, we varied the difference between K_{d2} and K_{d4} over a range of larger values until fitting yielded positive dissociation equilibrium constants for all reactions. The goodness of the fit decreased as the difference between K_{d2} and K_{d4} increased, so our final fit represents both the best fit to the data with positive dissociation equilibrium constants for all reactions and a lower limit for the value of K_{d4}. The low affinity of profilin-ADP-actin for barbed ends results from slow association of profilin-ADP-actin with barbed ends. The upper limit of the association rate constant is 10-fold lower than that for free ADP-actin binding to barbed ends.

The interactions of ADP-actin with profilin differ qualitatively from AMP-PNP-actin and ADP-P_i-actin. The affinity of free profilin for ADP-actin barbed ends is 40-fold greater than the affinity of profilin-ADP-actin for barbed ends, while the opposite is true for the interaction of profilin with AMP-PNP-actin or ADP-P_i-actin monomers and barbed ends. This is reflected in the lower limit for the dissociation equilibrium constant of profilin-ADP-actin on barbed ends (K_{d4}), which represents an affinity approximately 8-fold less than for profilin-AMP-PNP-actin and 20-fold less than for ADP-P_i-actin binding to barbed ends.

Our analysis yielded a higher affinity of profilin for ADP-actin barbed ends (K_{d3} = 0.9 μM) than reported by Jegou and coworkers (20) (K_{d3} = 28.1 μM). This group obtained their binding constant by fitting a hyperbolic curve to the dependence of the rates of depolymerization of filaments assembled from Mg-ADP-actin on the concentrations of profilin without actin monomers. However, profilin-stimulated filament depolymerization involves two sequential reactions: profilin binding to the barbed end followed by profilin-actin dissociation from the barbed end. Thus the binding constant obtained from their fitting does not correspond to one reaction. Instead their fitting parameter is a combination of binding constants for profilin on barbed ends (K_{d3} = 0.9 μM in our work) and profilin-actin on barbed ends (K_{d4} = 36.7 μM in our work). In a separate study, Kinosian et al. (15) assumed that profilin binds ADP-actin monomers and barbed ends with the same association rate constant of 15 $\mu M^{-1}s^{-1}$. Although our data analysis does not produce an association rate constant for profilin binding to barbed ends, their assumption led them to estimate a K_d of 20 μM for profilin-actin binding to barbed ends, which is similar to our measurement.

We observed a slower depolymerization rate for ADP-actin with saturating profilin than Jegou and coworkers (20). However, we agree with them that the rate of depolymerization of filaments assembled from ATP-actin increases over time in the presence of high concentrations of profilin (Supplemental Figure S2). The fastest dissociation rate in our experiment (−32 subunits/s in 125 μM profilin) approached the rate of −41 subunits/s observed by Jegou and coworkers for ADP-actin depolymerization in 80 μM profilin. As they suggested, this rate might correspond to the depolymerization of ADP-actin subunits that had hydrolyzed and dissociated phosphate. The differing affinities of profilin for barbed ends polymerized from AMP-PNP, ADP-P_i and ADP-actin suggest that filaments with each type of bound nucleotide have novel conformations (see below). It is also possible that nucleotide heterogeneity of the ends of ageing filaments polymerized from ATP-actin might make them less stable than homogeneous ADP-P_i or ADP-actin filament ends.

We draw the same conclusions from our thermodynamic analysis about the affinities of profilin and profilin-actin for barbed ends if we use our value of −12 subunits/s or Jegou's value of −41 subunits/s for the rate of profilin-ADP-actin dissociation from barbed ends. If we use an actin dissociation rate in 750 μM profilin of −41 subunits/s with our other data on ADP-actin (Fig. 3C), the best fit gives a K_{d3} of 14.4 μM and a K_{d4} of 68.5 μM (not shown). This affinity (K_{d4}) of profilin-ADP-actin monomers for barbed ends is weaker by only a factor of two compared with the fit to our data. Similarly, calculation of the association rate constant for profilin-ADP-actin binding to barbed ends (k_{4+}) produces a rate constant of 0.8 $\mu M^{-1}s^{-1}$, which is similar to the rate constant of 0.3 $\mu M^{-1}s^{-1}$ we obtained using our data and is still slower than free ADP-actin monomers binding to barbed ends. Including the faster profilin-actin dissociation rate in the analysis reduces the calculated affinity of profilin for ADP-bound barbed ends 15 fold. However, this lower affinity is still tighter than the affinity of profilin-ADP-actin monomers for barbed ends and does not affect our conclusions or the structural implications of our results (see below), given that it is the same order of magnitude as the calculated affinity of profilin for ADP-P_i-actin for barbed ends.

We conclude that profilin slows the elongation of filaments by ADP-actin through three mechanisms. First, profilin binds barbed ends with relatively high affinity (K_{d3} ~ 1 μM) where it blocks the association of actin monomers and profilin-actin. Second, profilin bound to a barbed end dissociates along with the terminal subunit at least twice as fast as an ADP-actin subunit. In addition ADP-actin bound to profilin associates with barbed ends much slower than free ADP-actin. The thermodynamics of the system are within 1 kcal/mol of detailed balance (Figure 1). However, as noted above, our fitting represents a lower limit for K_{d3} (the affinity of profilin for the barbed end). Fitting the data with a larger K_{d3} for the profilin binding the barbed end brings the system closer to equilibrium. For example, using K_{d3} = 5.2 μM results in a slightly weaker affinity of profilin-actin for barbed ends (K_{d4} = 50 μM) and brings the system to within 0.1 kcal/mol of detailed balance.

Structural analysis

We used molecular models to determine if profilin might bind to either or both the terminal and penultimate subunits at the barbed end of a filament. We used the co-crystal structure of actin monomer and bovine profilin (8) to dock human profilin on the two terminal subunits at the barbed end of an Oda (30) actin filament model (Figure 5). Since polymerized actin has a slightly flatter conformation than an actin monomer, profilin clashes directly with the subunit to which it is bound (Figure 5D). Specifically, we measured a total of 11 steric clashes (which we defined as contacts of less than 2.2 angstroms) involving atoms from 5 profilin residues (residues 59, 60 and 72–74) and 5 residues in actin subdomains 1 and 3 (residues 171, 173, 284, 286 and 375). Furthermore, profilin bound to the penultimate (n−1) subunit clashes with residues 223–228 and 259–272 in subdomain 4 of actin subunit n.

Similar models showed that both *S. pombe* profilin and *S. cerevisiae* profilin have similar clashes with adjacent subunits.

This analysis shows that profilin can only bind the barbed end of the terminal subunit n, and that profilin bound to this site precludes the addition of an actin subunit onto either the terminal or penultimate subunits. To avoid steric clashes with the bound profilin the conformation of this terminal subunit must be slightly less flat than the rest of the subunits in the filament. Profilin can come to be bound to the terminal subunit on the barbed end of a filament either by binding directly or binding as a profilin-actin complex. Profilin bound to the terminal subunit on the barbed end of a filament can either dissociate directly from this subunit or dissociate along with the terminal actin subunit as a profilin-actin complex (9).

Discussion

We undertook a thermodynamic analysis to determine rate and equilibrium constants for the various reactions involved in actin filament polymerization in the presence of profilin. Technical limitations had prevented direct measurement of these parameters in previous studies, but single filament visualization allowed us to measure elongation and shortening rates in the presence of a range of concentrations of profilin. Fitting a thermodynamic model to the profilin concentration dependence of these elongation rates yielded equilibrium constants and several rate constants for profilin and profilin-actin binding to filament barbed ends. We found that, although profilin has a higher affinity for ATP-actin monomers than ADP-actin monomers, it has a much higher affinity for the barbed ends of ADP-actin filaments than ATP-actin filaments or AMP-PNP-actin filaments. In addition, profilin binding to monomers has a 20-fold greater effect on AMP-PNP-actin monomer binding to AMP-PNP-filament barbed ends than for ADP-actin monomers and filaments.

Structural implications of our data analysis

The differences in the affinities of AMP-PNP- and ADP-bound barbed ends for profilin and profilin-actin strongly suggest that barbed end subunits have different conformations than monomers and that these conformations change upon nucleotide hydrolysis and phosphate release. Although experimental evidence of conformational dynamics of filamentous actin subunits in living cells is not available, we propose answers to three fundamental questions about these interactions based on our work with purified proteins.

Why does profilin have a higher affinity for actin monomers than barbed ends?—Regardless of the nucleotide bound to actin, profilin has a higher affinity for actin monomers than actin filament barbed ends. The most likely explanation is that ADP-actin subunits in filaments have subdomains 3 and 4 rotated relative to subdomains 1 and 2, resulting in flattening of the subunit relative to the monomer (30, 42). This rotation in the filament alters the orientation of the two halves of the profilin binding site located on the “bottoms” of subdomains 1 and 3 flanking the barbed end groove (8), creating minor steric clashes that can explain the lower affinity of profilin for barbed ends (Figure 5).

Thus, to bind profilin the actin subunit at the barbed end of an actin filament must take up at least transiently a different conformation from the average internal subunit. Conformational changes to accommodate profilin binding are most likely to occur within the terminal actin, since profilin is not known to populate different conformations. The well documented structural heterogeneity among the subunits of polymerized actin (43) suggests that they possess inherent flexibility that may contribute to profilin binding.

How does the bound nucleotide influence the affinity of profilin for barbed ends?—The nucleotide bound to actin monomers has only a small influence on the affinity

for profilin compared with the large impact of the bound nucleotide on the affinity of barbed ends for profilin. The affinities of ADP-actin monomers and barbed ends differ by only 4.5-fold, while profilin binds much more weakly to barbed ends than monomers of AMP-PNP-actin (2260-fold) and ADP-P_i-actin (102-fold). These huge differences in affinities suggest that the structures of the subunits at the barbed end of ADP-actin filaments may resemble actin monomers more closely than the terminal subunits of AMP-PNP-actin and ADP-P_i-actin filaments. We suggest that the absence of the γ-phosphate allows a terminal ADP-actin subunit greater freedom to assume monomer-like conformations that are favorable for binding profilin. Structures of barbed ends with different nucleotides (comparable to the cryoelectron microscopy structure of pointed ends (44)) should be very informative.

Why do barbed ends have a higher affinity for actin monomers than profilin-actin?—Bound profilin weakens the affinity of actin subunits for barbed ends. Although the nucleotide binding cleft may be open or closed in crystal structures of actin monomers bound to profilin (8, 45, 46), none of these structures has subdomains 3 and 4 rotated relative to subdomains 1 and 2 as observed in filaments (30, 42). This suggests that bound profilin may limit the conformational flexibility of actin monomers and reduce their ability to undergo the conformational changes associated with polymerization. For all three nucleotide states, bound profilin increases the dissociation rate constant of the terminal subunit, suggesting that profilin bound to the terminal subunit favors a conformation that compromises interfacial contacts with subunits n−1 and n−2.

The difference in the affinity of barbed ends for actin monomers and profilin-actin is much greater for AMP-PNP-actin than for ADP-P_i-actin and ADP-actin. This suggests that nucleotide hydrolysis and subsequent phosphate release alleviate some of the effects of profilin-binding on actin subunit conformational flexibility. However, owing to the low affinity of barbed ends for P_i (39), it is likely that some of the ADP-P_i-actin barbed ends observed in our experiments are really ADP-actin barbed ends. This makes it difficult to quantify the relative effects of nucleotide hydrolysis and phosphate release on barbed end affinity.

Profilin bound to ADP-actin monomers also slows their association with barbed ends. Even though the profilin-binding sites of ADP-actin monomers and barbed ends resemble each other, it follows from detailed balance that the relatively tightly bound profilin will compromise association of monomeric ADP-actin with barbed ends. This may be achieved via an allosteric effect on subunits 1 and 2, which associate with the barbed end, and have been demonstrated to populate a variety of conformational modes in filaments (43).

Effect of profilin on elongation of actin filament barbed ends by ATP-actin

Barbed end elongation rates with 1.5 μM Mg-ATP-actin monomers were close to zero with ~60 μM profilin (Figure 4A), a profilin concentration in between the concentrations required to stop elongation of barbed ends by Mg-AMP-PNP- and Mg-ADP-P_i-actin monomers (Figure 4B, C). Profilin concentrations >75 μM caused barbed ends to shorten in the presence of Mg-ATP-actin monomers. Given the low concentration of total ATP-actin (1.5 μM) and its high affinity for profilin (K_{d1} = 0.1 μM), most ATP-actin monomers were bound to profilin at all profilin concentrations (10–150 μM) tested, so the main species that varied with total profilin concentration was the free profilin concentration. Because of the heterogeneity in the nucleotide composition of the filaments, we did not perform a thermodynamic analysis of the elongation data. However, we estimate that the free profilin titrated a species with an affinity for barbed ends that lies in the range of 10–226 μM (or between the affinity of profilin for barbed ends composed of Mg-ADP-P_i-actin and Mg-AMP-PNP-actin). Further, because filaments elongated in the presence of profilin

concentrations where all of the actin was likely to be bound to profilin (10–60 μM total profilin), Mg-ATP-actin-profilin complexes must have a higher affinity for barbed ends than free profilin. We estimate this affinity to be in the low micromolar range, as observed for Mg-ADP-P_i-actin and Mg-AMP-PNP-actin.

The energetics of filament elongation in the presence of profilin have puzzled the field since it was discovered that actin monomers saturated with profilin can elongate barbed ends (9). Investigators proposed that binding reactions provide the energy for polymerization of ATP-actin (15, 18) or that energy from ATP hydrolysis is required to balance the reaction (47). However, because the thermodynamic parameters we obtain from our data analysis are balanced for AMP-PNP-actin, ADP-P_i-actin and ADP-actin monomers, we hypothesize that the four reactions described above are balanced during ATP-actin polymerization with profilin, regardless of the age (and therefore nucleotide state) of the subunits at the barbed end, and that no additional energy is required for polymerization.

Implications for profilin function in vivo

Our results fill in several missing kinetic and thermodynamic parameters that are required to explain how profilin influences actin polymerization in cells. At cellular profilin concentrations in the range of 100 μM most unpolymerized actin is bound to profilin (13) and little free profilin is available to bind barbed ends. The high concentration of profilin-actin adds to free barbed ends and also promotes elongation of barbed ends associated with a formin by binding to the FH1 domain and being delivered rapidly the end of the filament (28, 48). If a filament is severed, exposing a barbed end with terminal ADP-actin subunits, free profilin might bind and promote dissociation of subunits at a rate (12 s^{-1}) faster than dissociation of ADP-actin from a free end. However, given ~100 μM profilin-ATP-actin in the cytoplasm (13) the filament will grow until it is capped. In cells with thymosin-β4, that protein sequesters part of the unpolymerized actin (47, 49), adding another factor to consider.

Supplementary Material

Refer to Web version on PubMed Central for supplementary material.

Acknowledgments

This work was supported by NIH research grant GM-026338 and a fellowship from the Leukemia and Lymphoma Society. The authors thank Aaron G. Downs for carrying out preliminary experiments, Christopher Jurgenson and Mark Zweifel for help with molecular graphics and Julien Berro for help with the thermodynamic analysis.

References

1. Birbach A. Profilin, a multi-modal regulator of neuronal plasticity. Bioessays. 2008; 30:994–1002. [PubMed: 18798527]
2. Carlsson L, Nyström LE, Sundkvist I, Markey F, Lindberg U. Actin polymerizability is influenced by profilin, a low molecular weight protein in non-muscle cells. J Mol Biol. 1977; 115:465–483. [PubMed: 563468]
3. Markey F, Larsson H, Weber K, Lindberg U. Nucleation of actin polymerization from profilactin opposite effects of different nuclei. Biochim Biophys Acta. 1982; 704:43–51. [PubMed: 7201325]
4. Tseng PC, Pollard TD. Mechanism of action of Acanthamoeba profilin: demonstration of actin species specificity and regulation by micromolar concentrations of MgCl2. J Cell Biol. 1982; 94:213–218. [PubMed: 7119015]
5. Tobacman LS, Brenner SL, Korn ED. Effect of *Acanthamoeba* profilin on the pre-steady state kinetics of actin polymerization and on the oncentration of F-actin at steady state. J Biol Chem. 1983; 258:8806–8812. [PubMed: 6863311]

6. Pollard TD, Cooper JA. Quantitative analysis of the effect of Acanthamoeba profilin on actin filament nucleation and elongation. Biochemistry. 1984; 23:6631–6641. [PubMed: 6543322]
7. Vandekerckhove J, Kaiser DA, Pollard TD. Acanthamoeba actin and profilin can be crosslinked between glutamic acid 364 of actin and lysine 115 of profilin. J Cell Biol. 1989; 109:619–626. [PubMed: 2569469]
8. Schutt CE, Myslik JC, Rozycki MD, Goonesekere NC, Lindberg U. The structure of crystalline profilin-beta-actin. Nature. 1993; 365:810–816. [PubMed: 8413665]
9. Yarmola EG, Bubb MR. How depolymerization can promote polymerization: the case of actin and profilin. Bioessays. 2009; 31:1150–1160. [PubMed: 19795407]
10. Tilney LG, Bonder EM, Coluccio LM, Mooseker MS. Actin from Thyone briareus sperm assembles on only 1 end of an actin filament: a behavior regulated by profilin. J Cell Biol. 1983; 97:112–142. [PubMed: 6863386]
11. Hill TL. Length dependence of rate constants for end-to-end association and dissociation of equilibrium linear aggregates. Biophys J. 1983; 44:285–288. [PubMed: 6652219]
12. Gutsche-Perelroizen I, Lepault J, Ott A, Carlier MF. Filament assembly from profilin-actin. J Biol Chem. 1999; 274:6234–6243. [PubMed: 10037710]
13. Kaiser DA, Vinson VK, Murphy DB, Pollard TD. Profilin is predominantly associated with monomeric actin in Acanthamoeba. J Cell Sci. 1999; 112(Pt 21):3779–3790. [PubMed: 10523513]
14. Kang F, Purich DL, Southwick FS. Profilin promotes barbed-end actin filament assembly without lowering the critical concentration. J Biol Chem. 1999; 274:36963–36972. [PubMed: 10601251]
15. Kinosian HJ, Selden LA, Gershman LC, Estes JE. Actin filament barbed end elongation with nonmuscle MgATP-actin and MgADP-actin in the presence of profilin. Biochemistry. 2002; 41:6734–6743. [PubMed: 12022877]
16. Kinosian HJ, Selden LA, Gershman LC, Estes JE. Non-muscle actin filament elongation from complexes of profilin with nucleotide-free actin and divalent cation-free ATP-actin. Biochemistry. 2004; 43:6253–6260. [PubMed: 15147209]
17. Lal AA, Korn ED. Reinvestigation of the inhibition of actin polymerization by profilin. J Biol Chem. 1985; 260:10132–10138. [PubMed: 4019504]
18. Pring M, Weber A, Bubb MR. Profilin-actin complexes directly elongate actin filaments at the barbed end. Biochemistry. 1992; 31:1827–1836. [PubMed: 1737036]
19. Bubb MR, Yarmola EG, Gibson BG, Southwick FS. Depolymerization of actin filaments by profilin. Effects of profilin on capping protein function. J Biol Chem. 2003; 278:24629–24635. [PubMed: 12730212]
20. Jegou A, Niedermayer T, Orban J, Didry D, Lipowsky R, Carlier MF, Romet-Lemonne G. Individual actin filaments in a microfluidic flow reveal the mechanism of ATP hydrolysis and give insight into the properties of profilin. PLoS Biol. 2011; 9:e1001161. [PubMed: 21980262]
21. MacLean-Fletcher S, Pollard TD. Identification of a factor in conventional muscle actin preparations which inhibits actin filament self-association. Biochem Biophys Res Commun. 1980; 96:18–27. [PubMed: 6893667]
22. Houk TW Jr, Ue K. The measurement of actin concentration in solution: a comparison of methods. Anal Biochem. 1974; 62:66–74. [PubMed: 4473917]
23. Kellogg DR, Mitchison TJ, Alberts BM. Behaviour of microtubules and actin filaments in living Drosophila embryos. Development. 1988; 103:675–686. [PubMed: 3248521]
24. Pollard TD. Polymerization of ADP-actin. J Cell Biol. 1984; 99:769–777. [PubMed: 6540783]
25. Fedorov AA, Pollard TD, Almo SC. Purification, characterization and crystallization of human platelet profilin expressed in Escherichia coli. J Mol Biol. 1994; 241:480–482. [PubMed: 8064860]
26. Kaiser DA, Goldschmidt-Clermont PJ, Levine BA, Pollard TD. Characterization of renatured profilin purified by urea elution from poly-L-proline agarose columns. Cell Motil Cytoskeleton. 1989; 14:251–262. [PubMed: 2611892]
27. Lu J, Pollard TD. Profilin binding to poly-L-proline and actin monomers along with ability to catalyze actin nucleotide exchange is required for viability of fission yeast. Mol Biol Cell. 2001; 12:1161–1175. [PubMed: 11294914]

28. Paul AS, Pollard TD. The role of the FH1 domain and profilin in formin-mediated actin-filament elongation and nucleation. Curr Biol. 2008; 18:9–19. [PubMed: 18160294]
29. Kuhn JR, Pollard TD. Real-time measurements of actin filament polymerization by total internal reflection fluorescence microscopy. Biophys J. 2005; 88:1387–1402. [PubMed: 15556992]
30. Oda T, Iwasa M, Aihara T, Maeda Y, Narita A. The nature of the globular- to fibrous-actin transition. Nature. 2009; 457:441–445. [PubMed: 19158791]
31. Krissinel E, Henrick K. Secondary-structure matching (SSM), a new tool for fast protein structure alignment in three dimensions. Acta Crystallogr D Biol Crystallogr. 2004; 60:2256–2268. [PubMed: 15572779]
32. Winn MD, Ballard CC, Cowtan KD, Dodson EJ, Emsley P, Evans PR, Keegan RM, Krissinel EB, Leslie AG, McCoy A, McNicholas SJ, Murshudov GN, Pannu NS, Potterton EA, Powell HR, Read RJ, Vagin A, Wilson KS. Overview of the CCP4 suite and current developments. Acta Crystallogr D Biol Crystallogr. 2011; 67:235–242. [PubMed: 21460441]
33. Sanner MF, Olson AJ, Spehner JC. Reduced surface: an efficient way to compute molecular surfaces. Biopolymers. 1996; 38:305–320. [PubMed: 8906967]
34. Kraulis PJ. MOLSCRIPT: A program to produce both detailed and schematic plots of protein structures. Journal of Applied Crystallography. 1991; 24:946–950.
35. Merritt EA, Bacon DJ. Raster3D: photorealistic molecular graphics. Methods Enzymol. 1997; 277:505–524. [PubMed: 18488322]
36. Kinosian HJ, Selden LA, Gershman LC, Estes JE. Interdependence of profilin, cation, and nucleotide binding to vertebrate non-muscle actin. Biochemistry. 2000; 39:13176–13188. [PubMed: 11052670]
37. Vinson VK, De La Cruz EM, Higgs HN, Pollard TD. Interactions of Acanthamoeba profilin with actin and nucleotides bound to actin. Biochemistry. 1998; 37:10871–10880. [PubMed: 9692980]
38. Amann KJ, Pollard TD. Direct real-time observation of actin filament branching mediated by Arp2/3 complex using total internal reflection fluorescence microscopy. Proc Natl Acad Sci U S A. 2001; 98:15009–15013. [PubMed: 11742068]
39. Fujiwara I, Vavylonis D, Pollard TD. Polymerization kinetics of ADP- and ADP-Pi-actin determined by fluorescence microscopy. Proc Natl Acad Sci U S A. 2007; 104:8827–8832. [PubMed: 17517656]
40. Pollard TD. Rate constants for the reactions of ATP- and ADP-actin with the ends of actin filaments. J Cell Biol. 1986; 103:2747–2754. [PubMed: 3793756]
41. Niedermayer T, Jegou A, Chieze L, Guichard B, Helfer E, Romet-Lemonne G, Carlier MF, Lipowsky R. Intermittent depolymerization of actin filaments is caused by photo-induced dimerization of actin protomers. Proc Natl Acad Sci U S A. 2012; 109:10769–10774. [PubMed: 22699501]
42. Fujii T, Iwane AH, Yanagida T, Namba K. Direct visualization of secondary structures of F-actin by electron cryomicroscopy. Nature. 2010; 467:724–728. [PubMed: 20844487]
43. Galkin VE, Orlova A, Schroder GF, Egelman EH. Structural polymorphism in F-actin. Nat Struct Mol Biol. 2010; 17:1318–1323. [PubMed: 20935633]
44. Narita A, Oda T, Maeda Y. Structural basis for the slow dynamics of the actin filament pointed end. Embo J. 2011; 30:1230–1237. [PubMed: 21378753]
45. Chik JK, Lindberg U, Schutt CE. The structure of an open state of beta-actin at 2.65 A resolution. J Mol Biol. 1996; 263:607–623. [PubMed: 8918942]
46. Ferron F, Rebowski G, Lee SH, Dominguez R. Structural basis for the recruitment of profilin-actin complexes during filament elongation by Ena/VASP. Embo J. 2007; 26:4597–4606. [PubMed: 17914456]
47. Pantaloni D, Carlier MF. How profilin promotes actin filament assembly in the presence of thymosin beta 4. Cell. 1993; 75:1007–1014. [PubMed: 8252614]
48. Kovar DR, Harris ES, Mahaffy R, Higgs HN, Pollard TD. Control of the assembly of ATP- and ADP-actin by formins and profilin. Cell. 2006; 124:423–435. [PubMed: 16439214]
49. Cassimeris L, Safer D, Nachmias VT, Zigmond SH. Thymosin beta4 sequester the majority of G-actin in resting human polymorphonuclear leukocytes. J Cell Biol. 1992; 119:1261–1270. [PubMed: 1447300]

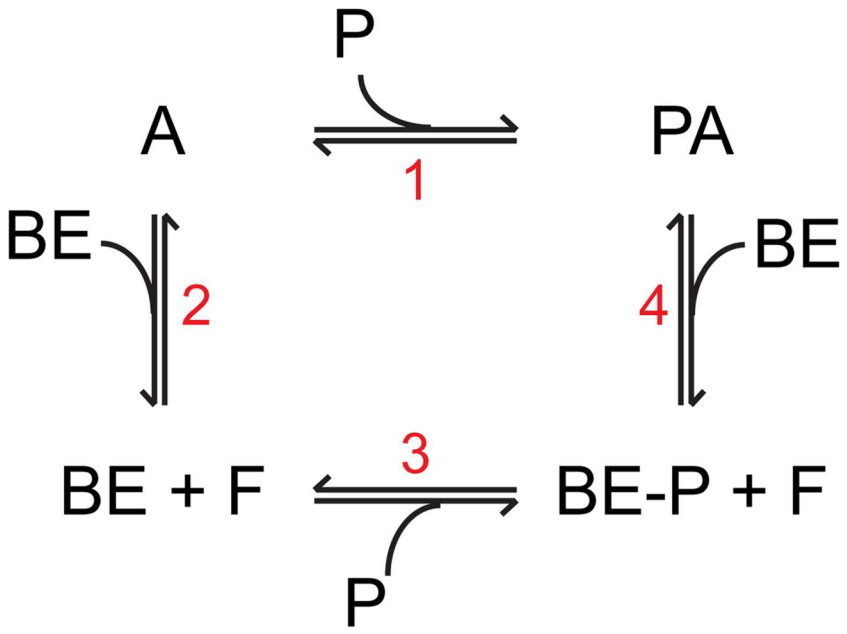

Figure 1.

Thermodynamic scheme of actin filament elongation in the presence of profilin. Four reactions are depicted and labeled as follows: (1) reaction of profilin (P) with an actin monomer (A); (2) reaction of an actin monomer with the barbed ends of a filament (BE); (3) reaction of profilin with the barbed end of a filament; and (4) reaction of the profilin-actin complex (PA) with the barbed end of a filament. “F” represents the newly incorporated filamentous subunit upon actin or profilin-actin binding to the barbed end. “BE-P” represents the profilin-bound barbed end. To satisfy a detailed balance, the sum of the free energies of reactions 1 and 4 must be equal to the sum of the free energies of reactions 2 and 3. Table 2 lists the thermodynamic and kinetic parameters for AMP-PNP-actin, ADP-P_i-actin and ADP-actin.

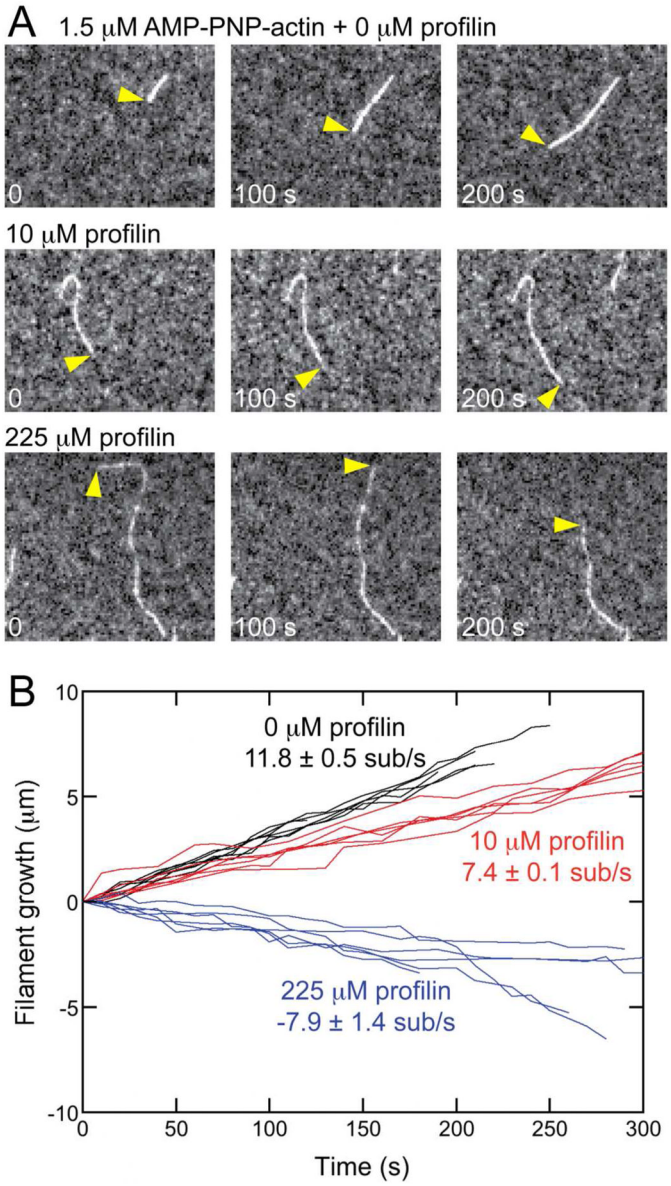

Figure 2.

Effect of profilin on barbed end elongation of Mg-AMP-PNP-actin filaments. Polymerization conditions: 10 mM imidazole (pH 7.0), 50 mM KCl, 1 mM $MgCl_2$, 1 mM EGTA, 50 mM DTT, 0.37 mM AMP-PNP, 0.02 mM $CaCl_2$, 15 mM glucose, 0.02 mg/ml catalase, 0.1 mg/ml glucose oxidase and 0.5% methylcellulose (4,000 cP at 2% (w/v)). Data were collected with total internal reflection fluorescence microscopy. (A) Time-series of images of 1.5 μM AMP-PNP-actin (20% Alexa 488-labeled) filaments growing in the presence of a range of concentrations of human profilin 1. Yellow arrowheads denote barbed ends. (B) Time courses of the growth of six representative filament barbed ends in the presence of 1.5 μM AMP-PNP-actin (20% Alexa 488-labeled) and profilin concentrations of 0 (black lines), 10 μM (red lines) or 225 μM (blue lines).

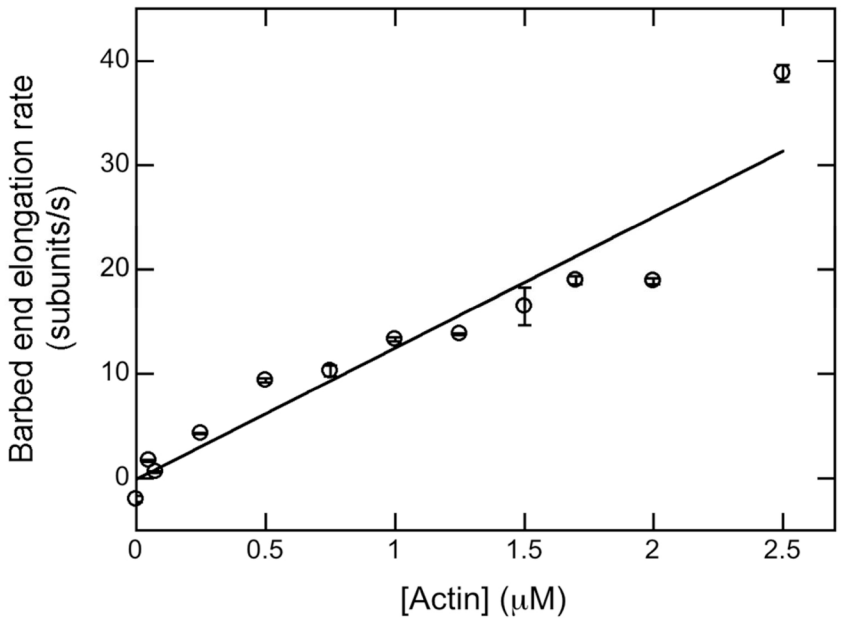

Figure 3.

Dependence of the elongation rates of AMP-PNP-actin filaments on the concentration of AMP-PNP-actin monomers. Growth of filaments was observed by total internal reflection fluorescence microscopy with concentrations of AMP-PNP-actin (20% Alexa-488-labeled) from 50 nM to 2.5 μM and in microscopy buffer with 0.37 mM AMP-PNP. Filament seeds were grown from 1.5 μM AMP-PNP-actin monomers in the observation chamber, followed by a wash and replacement with AMP-PNP-actin monomers. Error bars are 1 standard error of the mean elongation rate of at least 10 filaments.

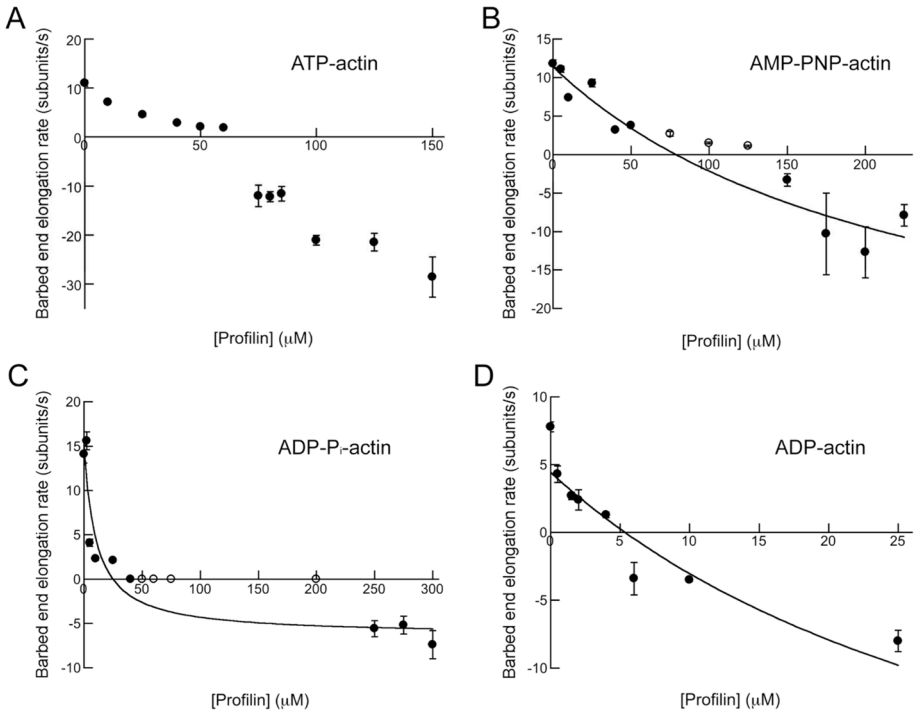

Figure 4.

Dependence of barbed end elongation rates by Mg-ATP-, Mg-AMP-PNP-, Mg-ADP-P_i- and Mg-ADP-actin monomers on the concentration of profilin 1. Data were collected by total internal reflection fluorescence microscopy. Error bars are standard errors of the mean elongation rates of at least 10 filaments. The smooth curves are fits to the filled data points with the model described in the text. The open data points were masked in these fits. (A) Conditions for Mg-ATP-actin monomers: 1.5 μM ATP-actin (20% Alexa-488-labeled), 0.2 mM ATP and a range of concentrations of profilin in microscopy buffer. (B) Conditions for Mg-AMP-PNP-actin monomers: 1.5 μM AMP-PNP-actin (20% Alexa-488-labeled), 0.37 mM AMP-PNP and a range of concentrations of profilin in microscopy buffer. (C) Conditions for Mg-ADP-P_i-actin monomers: 4 μM Mg-ADP-P_i-actin (20% Alexa-488-labeled), 0.3 mM ADP, 20 units/mL hexokinase, 12.5 mM potassium phosphate and a range of concentrations of profilin in microscopy buffer. The polymerization buffer contained 25 mM KCl instead of 50 mM to compensate for the additional K^+ ions. (D) Conditions for Mg-ADP-actin monomers: 5.0 μM Mg-ADP-actin (20% Alexa-488-actin), 0.3 mM ADP and 20 units/mL hexokinase and a range of concentrations of profilin in microscopy buffer.

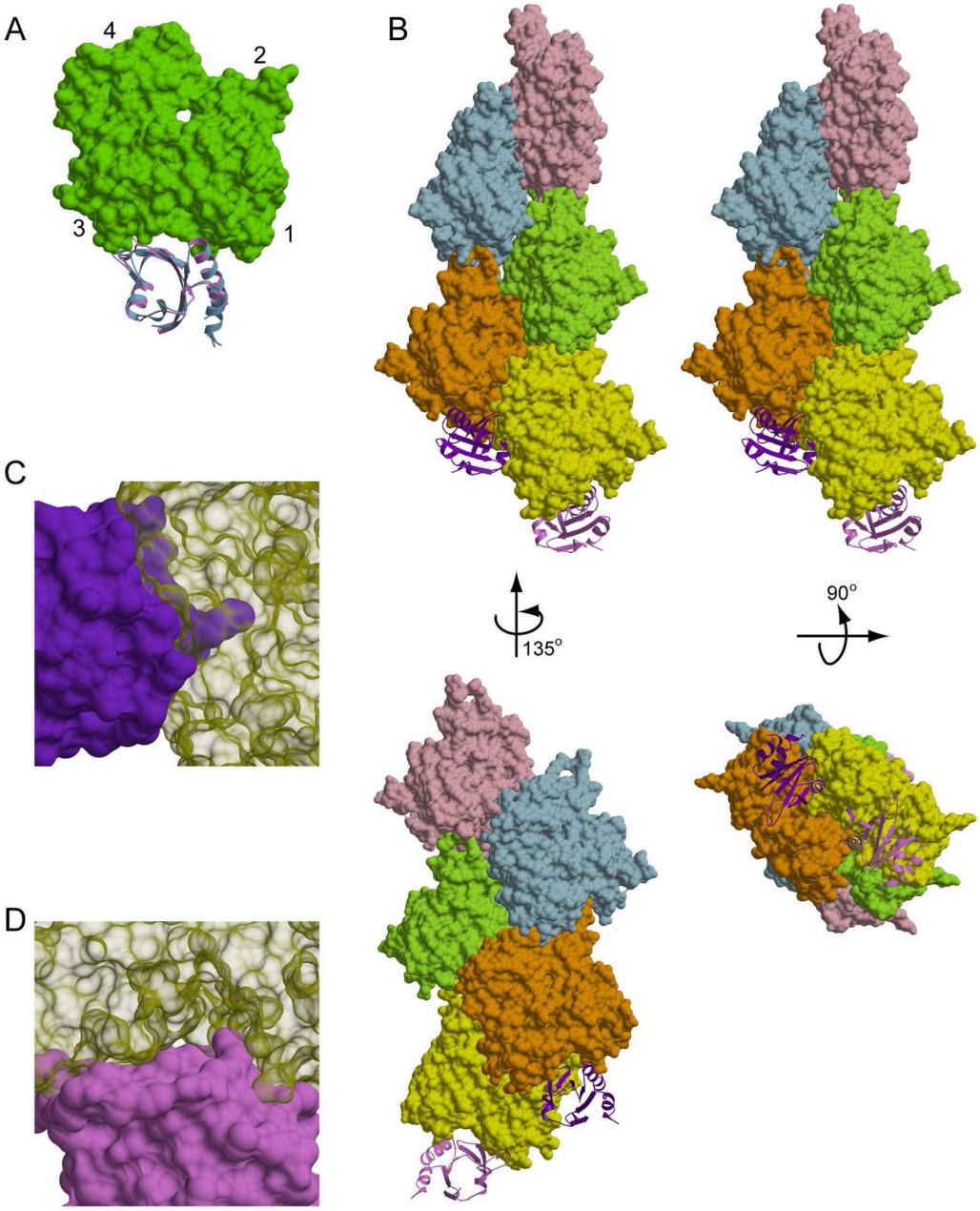

Figure 5.

Molecular models showing steric clashes produced by profilin binding to the terminal subunits of both long-pitch helices (subunits n and n−1) of an actin filament. Solvent excluded surface model of actin and ribbon diagrams of profilin are shown. (A) Superposition of human profilin (purple; pdb: 1FIK) onto the structure of bovine β-actin (green) bound with bovine profilin (blue; pdb: 1HLU). (B) (*Upper panels)* Stereo view of an Oda actin filament model (30) with human profilin I (dark purple and light purple) bound to the terminal subunits of each long-pitch helix (subunits n and n−1) as in (A). *(Lower panels)* Additional views of the filament and bound profilin molecules. (C) Detail of the clashes formed between profilin (dark purple) and subdomain 1 of actin subunit n (yellow) when profilin is bound to actin subunit n−1. Solvent excluded surfaces are shown (33). (D) Detail

of the profilin-actin interface at the terminal barbed end subunit (profilin, light purple; actin subunit n, yellow). Solvent excluded surfaces are shown (33).

Table 1

Initial rate of barbed end depolymerization (subunits s^{-1}) with zero or 750 μ profilin.

	ATP-actin	AMP-PNP-actin	ADP-P_i-actin	ADP-actin
No profilin	1.4 ± 0.8[b]	2.0 ± 0.3[a]	0.2 ± 0.1[c]	5.4 ± 0.14[c]
750 μM profilin	30.3 ± 3.3[a]	52.4 ± 4.9[a]	8.6 ± 1.1[a]	12.2 ± 2.8[a]

[a] Rates measured in this study. The ATP-actin rate is the initial depolymerization rate.

[b] See Pollard, 1986 (40)

[c] See Fujiwara et al., 2007 (39).

Table 2

Summary of reaction rates and affinities for AMP-PNP-, ADP-P_i-, ADP-actin and profilin.

	Reaction	AMP-PNP				ADP-P_i				ADP			
		k_+ ($\mu M^{-1}s^{-1}$)	k_- (s^{-1})	K_d (μM)	ΔG (kcal/mol)	k_+ ($\mu M^{-1}s^{-1}$)	k_+ ($\mu M^{-1}s^{-1}$)	K_d (μM)	ΔG (kcal/mol)	k_+ ($\mu M^{-1}s^{-1}$)	k_- (s^{-1})	K_d (μM)	ΔG (kcal/mol)
1	A + P ⇆PA	14[d]	1.3[d]	0.1[d]	9.5	14[d]	1.3[d]	0.1[d]	9.5	15.6[d]	2.6[d]	0.2[d]	9.1
2	A+BE ⇆BE+F	12.6[a]	0.09[a]	0.01[a]	10.9	3.4[e]	0.2[e]	0.06[e]	9.8	2.9[f]	5.0[f]	1.7[f]	7.9
3	BE+P⇆BE-P	n.d.[c]	n.d.[c]	226[b]	5.0	n.d.[c]	n.d.[c]	10.2[b]	6.8	n.d.[c]	n.d.[c]	0.9[b]	8.2
4	PA+BE⇆BE-P+F	11.4[b]	52.4[a]	4.6[b]	7.3	4.1[b]	8.6[a]	2.1[b]	7.7	0.3[b]	12.2[a]	36.7[b]	6.0

[a] Rates and affinities measured in this study.

[b] Rates and affinities extracted from our fitting analysis.

[c] Not determined.

[d] See Kinosian et al., 2000 (36). We assumed similar thermodynamics for profilin binding to ATP-actin, AMP-PNP-actin and ADP-P_i-actin monomers.

[e] See Fujiwara et al., 2007 (39).